Supporting Information

DOI: 10.1002/ ((please add manuscript number))
Article type: Research Article

Heteroatom-doped noble carbons tailored mixed matrix membrane with ultrapermeability for efficient CO_2 separation

Zhihong Tian,† Dongyang Li,† Weigang Zheng, Qishuo Chang, Yudong Sang, Feili lai, Jing Wang, Yatao Zhang*, Tianxi liu, Markus Antonietti*

Prof. Z. Tian
Engineering Research Center for Nanomaterials, Henan University, Kaifeng 475004, P. R. China.

Prof. D. Li, W. Zheng, Q. Chang, Y. Sang, Prof. J. Wang, Prof. Y. Zhang,
School of Chemical Engineering, Zhengzhou University, Zhengzhou 450001, P. R. China
Email: wang.jing@zzu.edu.cn； zhangyatao@zzu.edu.cn

Dr. F. Lai
Department of Chemistry, KU Leuven, Celestijnenlaan 200F, Leuven 3001, Belgium

Prof. T. Liu
Key Laboratory of Synthetic and Biological Colloids, Ministry of Education, School of Chemical and Material Engineering, Jiangnan University, Wuxi 214122, P. R. China.

Prof. M. Antonietti
Department of Colloid Chemistry, Max Planck Institute of Colloids and Interfaces, Potsdam 14476, Germany

† These authors contributed equally to the preparation of the manuscript

Keywords: Noble carbon, C_2N, CO_2 separation, mixed matrix membrane, PIM-1

Experimental section:

1. Materials Synthesis and Characterization:

Materials: For $C_2N_xO_{1-x}$ synthesis, 3,4,5-trihydroxy benzoic acid (Gallic acid) and urea were obtained from Sigma-Aldrich Co., Ltd. Anhydrous Zinc chloride ($ZnCl_2$) was purchased from Acros organics Co., Ltd. Hydrochloric acid (HCl) was supplied from Adamas Co., Ltd. For PIM-1 synthesis and membranes fabrication, 5,5',6,6'-tetrahydroxy-3,3,3',3'-tetramethyl-1,1'-spirobisindane (TTSBI, 97%) and 2,3,5,6-tetrafluoroterephthalonitrile (TFTPN, 98%) were purchased from TCI Co., Ltd and purified before used. Potassium carbonate (K_2CO_3, 99%) was purchased from Aladdin Co., Ltd. Methanol (MeOH, 99.9%), chloroform (analytical grade), and polyethylene glycol (PEG-200) were provided from Sinopharm Chemical Reagent Co., Ltd. Anhydrous N, N- dimethylacetamide (DMAc, analytical grade) was purchased from Adamas Co., Ltd. All reagents were used as received except for TTSBI and TFTPN.

Synthesis of $C_2N_xO_{1-x}$: A mixture of gallic acid (5 mmol), urea (15 mmol), and $ZnCl_2$ (in a weight ratio of precursor: salt of 1:8) was placed in a crucible and carbonized in N_2 under 500 ℃ for 3 h. After cooling down, the crude product was stirred with hydrochloric acid (1M) for 12 h. The resulting product was filtered and washed with deionized water to neutral pHand then dried at 80 ℃ for 24 hours.

Synthesis of PIM-1: PIM-1 was synthesized according to the reported literature, the synthetic process was briefly described below: a certain amount of TTSBI, TFBN, and DMAc was placed in a three-neck bottle and stirred until completely dissolved. Add a certain amount of potassium carbonate and then the mixture was stirred under an N_2 atmosphere at 155 °C for some time. Then, toluene was added to the bottle and continuously reacted for a certain time. The product was poured into methanol to obtain flocculent precipitate after cooling to room temperature and then filtered to obtain a yellow solid. The resultant polymer was dissolved in $CHCl_3$ and reprecipitated from MeOH three times for purification and then dried under vacuum at 80°C for 12 h.

Preparation of PIM-1/$C_2N_xO_{1-x}$ membranes and P-PIM-1/ $C_2N_xO_{1-x}$ membranes: PIM-1/$C_2N_xO_{1-x}$ MMMs were prepared as follows: PIM-1 powder was dissolved in chloroform to form PIM-1/$CHCl_3$ solution, and then filtered with 0.45 μm PTFE filter cartridge. The PIM-1 solution was added to the desired mass fraction of $C_2N_xO_{1-x}$ /$CHCl_3$ suspension and stirred for 24 h to form a mixed-matrix solution. The resulting solution was poured into a circular glass mold supported by a leveled glass plate after being sonicated for 2 h to remove the bubbles of the casting solution. The membrane was allowed to form by slow solvent evaporation for at least 24 h in a drying oven under ambient temperature. The resulting membrane was soaked in methanol for six hours and then heated at 50°C for 24 h under a high vacuum to remove any traces of residual solvent. The preparation method of PEG-treated PIM-1/$C_2N_xO_{1-x}$ membranes (P- PIM-1/$C_2N_xO_{1-x}$) is similar to PIM-1/$C_2N_xO_{1-x}$: a certain quality of PEG-200 (10%-60%) was added into $C_2N_xO_{1-x}$/$CHCl_3$ suspension and stirred for 6 h, then the PIM-1 solution was placed the above suspension and kept stirring. The dried membrane is soaked in methanol for 6 hours to remove the small molecule PEG from the membrane. The pristine PIM-1 membrane and P-PIM-1 membrane were fabricated via the same procedure.

Materials and structural characterizations: The crystalline structure of $C_2N_xO_{1-x}$ and PIM-1/$C_2N_xO_{1-x}$ MMMs was characterized by X-ray diffraction apparatus (XRD-6100, Shimadzu KRATOS corporation in Japan) in the range of 5-40° using Cu Kα radiation at 45 kV, 40 mA. The surface and the cross-section morphologies of MMMs were characterized by a scanning electron microscope (SEM, JSM-6700F). The chemical bonds and groups of $C_2N_xO_{1-x}$ and membranes were obtained by Fourier Transform Infrared spectroscopy (FTIR, Thermo Nicolet, USA). The Ar adsorption/desorption isotherms of $C_2N_xO_{1-x}$ particles and membranes were measured by a gas adsorption instrument (ASAP2460) at 77 K. The surface area of $C_2N_xO_{1-x}$ was calculated by the Brunauer-Emmett-Teller (BET) and pore size distribution was calculated by the NL-DFT method. Thermo gravimetric analysis (TGA) (TGA-50 Bruker) was conducted at a temperature range from 20 °C to 800 °C in a nitrogen atmosphere (the flow rate is 30 ml/min).

Gas permeation measurements: The breakthrough experience was conducted by a multi-component adsorption breakthrough curve analyzer (BSD-MAB). The adsorbent sample was pretreated by passing Ar at a flow rate of 10 sccm at 473 K for 2 h. During the experiment, the mixture gas (CO_2/N_2=10/90 vol%) was used as feed gas while Ar was used as the sweep gas. The experimental temperature was 300 K and column pressure was fixed at 1.3 bar.

breakthrough experiments. GC was used to analyze outlet gas composition until the gas composition reaches the feed. Detailed parameters are listed in Table. S1.

The single gas permeability test was conducted by a traditional constant volume device (FHM-PermCell-Lab, Suzhou Xinwang Membrane Technology Co., LTD) which is based on a different-pressure method, the bleed pressure was in the range from 1 bar to 5 bar in this work. To avoid errors, each membrane was averaged three times during the whole test.

The calculation formula of membrane permeability (P) is as follows:

$$P = \frac{273 \times 10^{10}}{760} \times \frac{V \cdot l}{A \cdot T\left(P_0 \times \frac{76}{14.7}\right)} \times \frac{dp}{dt} \#(1)$$

P is the gas permeability with the unit of Barrer (1 Barrer=1×10^{-10} cm^3 (STP) cm cm^{-2} s^{-1} $cmHg^{-1}$), V expresses the low-pressure chamber volume (cm^3), l represents the thickness of the tested membrane (cm), A expresses the active area of the tested membrane (cm^2), T is the testing temperature (K) and P_0 presents the pressure of upstream chamber (psi), where $\frac{dp}{dt}$(cmHg/s) is the rate of pressure increase in the downstream cavity of the low pressure.

The diffusion coefficient (*D*, cm^2/s) and solubility coefficient (*S*, cm^3 (STP)/cm^3 cmHg) can be calculated as follows:

$$D = \frac{l^2}{6\theta}\#(2)$$

$$S = \frac{P}{D}\#(3)$$

Where ϑ represents the gas lag time.

The gas selectivity for a membrane can be calculated by the formula:

$$\alpha_{CO_2/N_2} = \frac{P_{CO2}}{P_{N_2}}\#(4)$$

P_{CO_2} and P_{N_2} are the permeability of CO_2 and N_2 respectively.

The mixed-gas (CO_2/N_2, 10/90, v/v) permeability measurement was conducted by a generally constant pressure/variable volume system in a dry and humid environment. He was applied as sweeping gas to sweep the mixed gas into a gas chromatography. In the humid mixed-gas test, the mixed gas was saturated with vapor by bubbling through a water bottle at 35 °C and then passing an unfilled bottle at 25 °C to eliminate condensate. The sweeping gas was humidified at room temperature through a constant pressure humidifier in the humid mixed-gas test process. The permeate gas was analyzed by an online GC (GC-2014C) to determine the gas stream composition and gas selectivity for a membrane can be calculated by the formula:

$$\alpha_{CO_2/N_2} = \frac{P_{CO2}}{P_{N_2}}\#(5)$$

Molecular modeling and dynamics simulation: The model of PIM-1 and $C_2N_xO_{1-x}$ are built through a non-commercial software Xenoview[1] in this study, where the all-atom force field, PCFF[2], is applied to describe the non-bonded and bonded interactions. The partial charges are taken from Marcel Balçık et al.[3] However, the charges on $C_2N_xO_{1-x}$ is modified based on our previous study[4]. Molecular dynamics (MD) simulation is implemented through LAMMPS[5], where the equilibration protocol of PIM-1 and PIM-1/$C_2N_xO_{1-x}$ models follows the general heating-cooling strategy[6,7] and the details are listed as follows,

Step 1. Model PIM-1 and $C_2N_xO_{1-x}$ with PCFF, then pack them into amorphous cells with an initial density of 0.5-0.6 g/cm^3;

Step 2. Energy minimization to optimize the energy of amorphous cells;

Step 3. Repeat 6 cycles of heating (1ns, 600K) and cooling (1ns, 300K) at NPT ensemble (P=1 atm).

The cutoff of non-bonded interactions is set at 14Å, and the long-range VdW and electrostatic interactions are estimated through the tail correction and Ewald summation method, respectively. The time step, 1 fs, is employed to process time integration in the standard velocity-verlet algorithm. The temperature and pressure are controlled by the thermo- and barostats Nose-Hoover chains, respectively. As a result, the computed density of PIM-1 is 1.058±0.004 g/cm^3, which is close to the experimental data of 1.06-1.09 g/cm^3[8,9] and the reported simulation results of 1.046 g/cm^3[10] but is a bit lower than some simulations (≈1.001[3]). Note that the force field used in this study is an all-atoms model named PCFF, while Balçık et al. employed a united-atom model named TraPPE-UA, which properly decreased the packing density of the polymer. The equilibrated structure is then applied to calculate the FFV (fractional free volume). When using a probe radius of 0.43 Å and grid size of 0.5 Å, FFV≈22.05% is a bit higher than the experimental estimation (≈19.2%[11]) and close to the simulated result (≈22.8%[11]) by the Bondi method and is lower than some computation result (≈23.4%[12]) through the particle-insertion method, which does make sense properly due to the relative higher packing density in this study. PCFF was also employed to model CO_2 and N_2 in this study. The Grand Canonical Monte Carlo (GCMC) method[13] was used to compute the sorption performance of PIM-1 and PIM-1/$C_2N_xO_{1-x}$, where 3 ns and 1 ns Monte Carlo steps were employed in equilibration and production stages, respectively. MD simulation is then adopted to measure the diffusion performance of CO_2 and N_2, in which 20 ns NVT steps were run to fit the diffusion coefficient for each system. The computed gas sorption and diffusion coefficients with changing $C_2N_xO_{1-x}$ compositions are summarized in Table S1. The modeling and simulation methods are further validated by the same magnitude of gas solubility (~$O(10^{-1})$, cm^{3}cm^{-3}cmHg^{-1}) and diffusivity (~$O(10^{-7})$, cm^2/s) as the previous experiments[14-15] and simulations[3,16]. Because of different force field parameters and system sizes applied in simulation, the difference in overall permeability is acceptable within the same magnitude. Unfortunately, Considering the lack of experimental data on $C_2N_xO_{1-x}$, the validation of the molecular model seems difficult in this study. It deserves to note that this study aims to make a qualitative comparison of material performance changes with $C_2N_xO_{1-x}$ compositions between the simulation and experiment instead of model investigation and modification. The composition of PIM-1, $C_2N_xO_{1-x,}$ and gas molecules in each molecular dynamics simulation are summarized in Tab.S2.

RDF calculation: The function used to calculate RDF can be found every textbook and popularly used to evaluate the strong interactions[17], and in this study, 1 ns NVT simulation was ran and 100 configurations were collected to make statistics of g(r). All the computed g(r) is observed to converge to 1 within a distance of 14 Å, ensuring the validity and accuracy of calculation.

Binding energy calculation: Binding energy is calculated in the following form[18],

$$\Delta E_{binding} = E_{PIM-1/C2NxO1-x} - E_{PIM-1} - E_{C2NxO1-x}$$

where $E_{PIM-1/C2NxO1-x}$, E_{PIM-1} and $E_{C2NxO1-x}$ represent the total energy of mixture, PIM-1 chains and $C_2N_xO_{1-x}$, respectively, which are directly collected from the equilibrated configuration.

FFV calculation: Fractional free volume is calculated in the following form,

$$f = \frac{V_1 - V_0}{V_1}$$

where *V_1* stands for the total volume of the simulated membrane (pure PIM-1 or PIM-1/ $C_2N_xO_{1-x}$ mixture), and *V_0* represents the volume occupied by a membrane and is 1.3 times of the van der Waals volume. In this study, the probe radius is chosen to be 0.43Å and the grid size is 0.5 Å. The snapshot of FFV for pure PIM-1 and PIM-1/ $C_2N_xO_{1-x}$ mixture are shown in Fig. S1 and Fig.7, respectively.

Part I: Supporting Figures

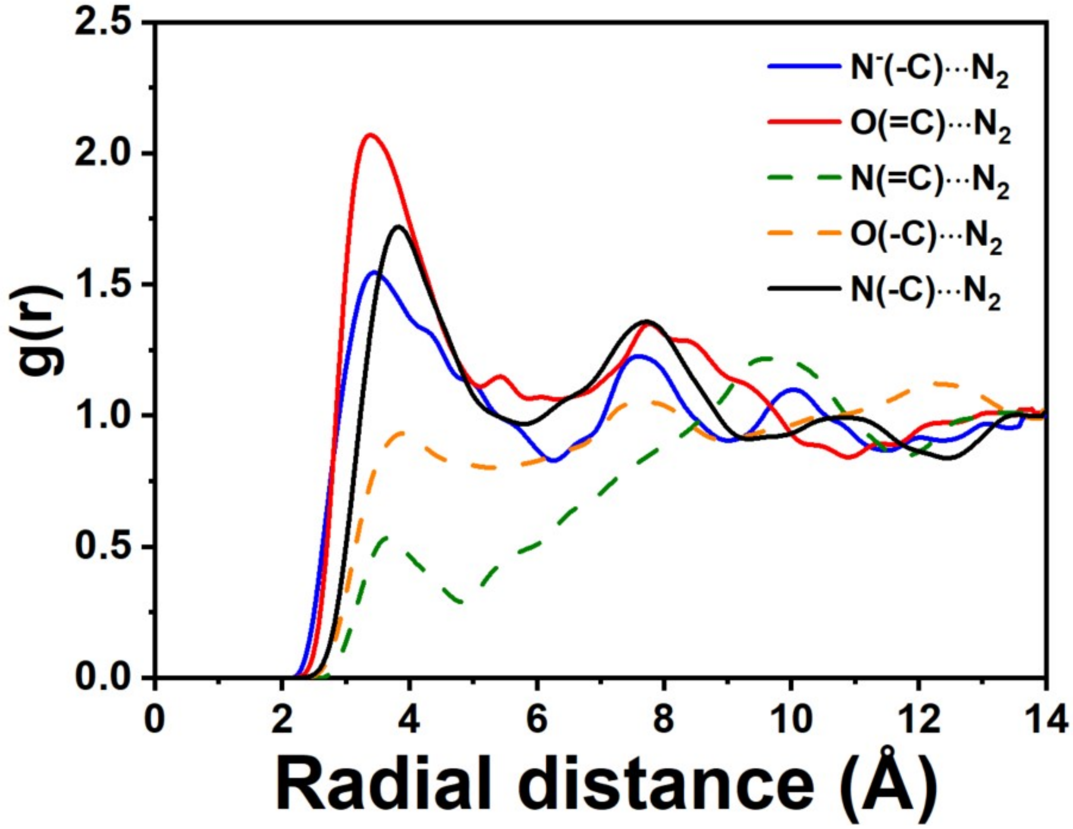

Fig. S1 RDFs between negatively charged heteroatoms, $N^-(-C)$, O(=C), N(=C), O(-C), and N(-C) on $C_2N_xO_{1-x}$ and positively charged C(=O) atom on N_2

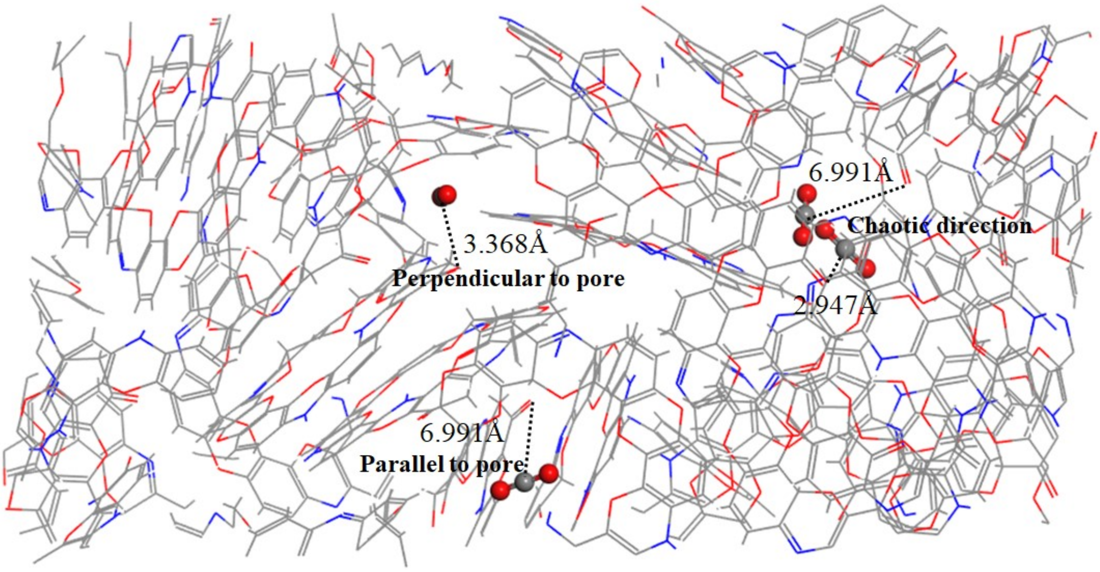

Fig. S2 Snapshot of CO_2 adsorbed in $C_2N_xO_{1-x}$, dashed line and number describes the viewable distance between O(=C) on $C_2N_xO_{1-x}$ with CO_2.

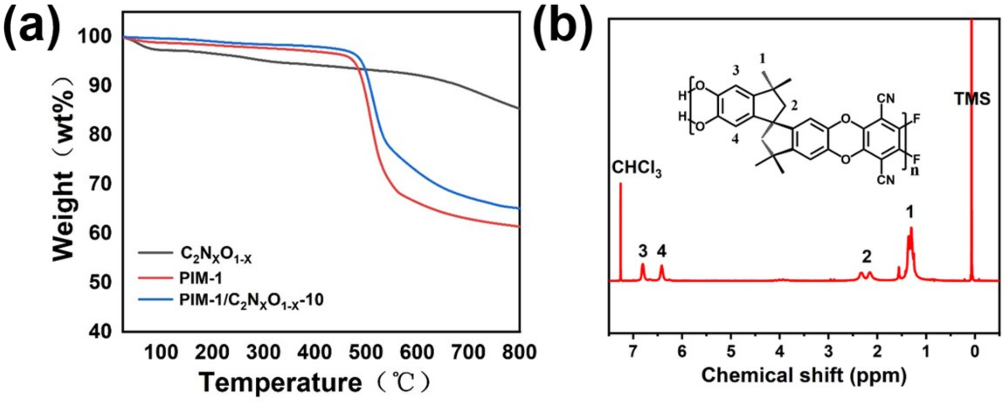

Fig. S3 a) Thermogravimetric analysis of $C_2N_xO_{1-x}$, PIM-1 and PIM-1/$C_2N_xO_{1-x}$-10 membranes. b) ^1H (400 MHz) NMR spectrum of PIM-1

The weight loss for PIM-1 and PIM-1/$C_2N_xO_{1-x}$ membranes are less than 2.5 % before 500 ^oC. The chemical structures of PIM-1 were determined by ^1H NMR spectroscopy. The ^1H NMR spectrum shown in Fig. R2 matched with the ^1H NMR spectrum reported by the literature, indicating the successful preparation of PIM-1.[19-23] Besides, no impurity peaks were observed except those for TMS and $CDCl_3$, indicating the high purity of PIM-1.

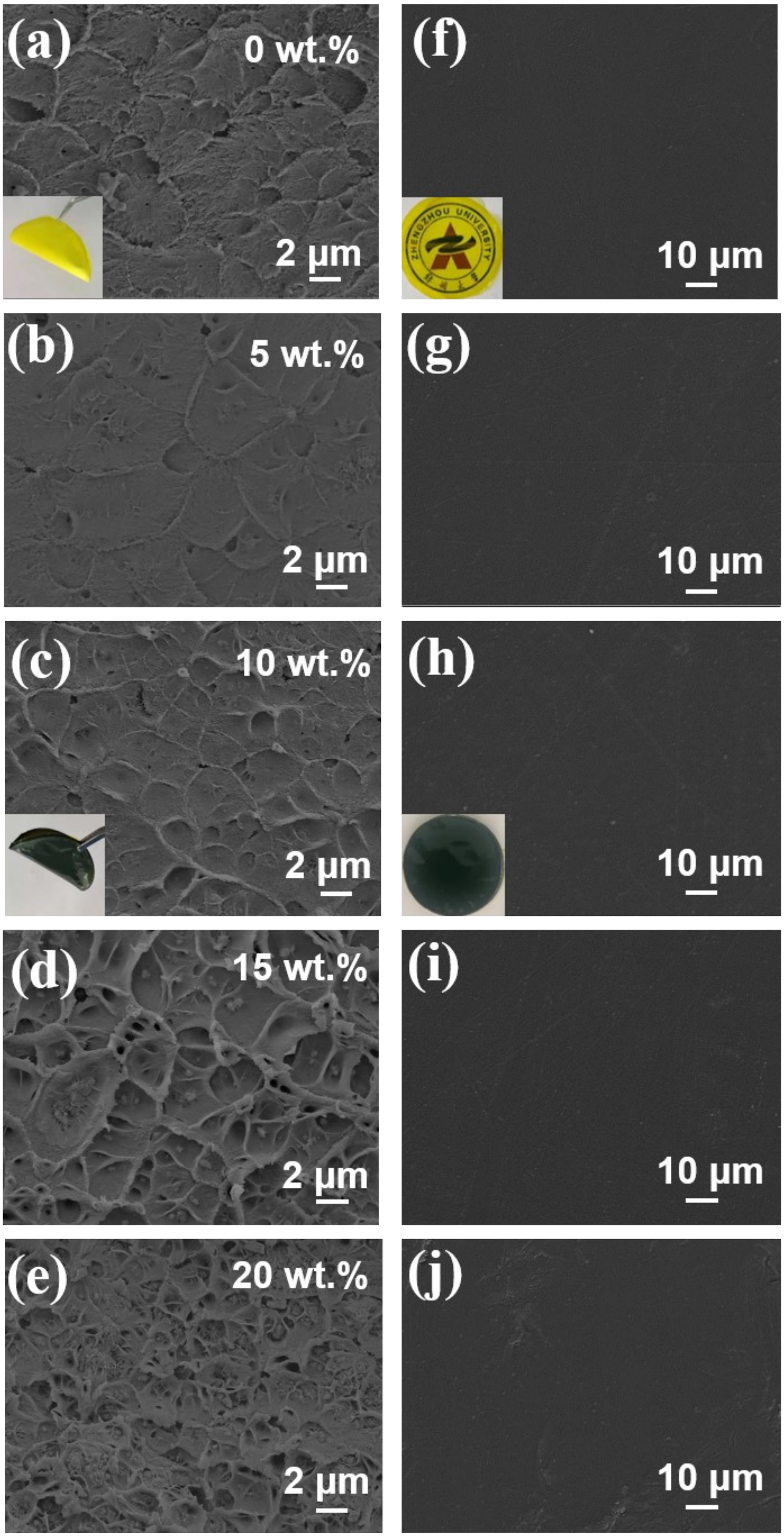

Fig. S4 The surface morphology SEM of a, f) PIM-1 membrane, b, g) PIM-1/$C_2N_xO_{1-x}$-5 membrane, c, h) PIM-1/$C_2N_xO_{1-x}$-10 membrane, d, i) PIM-1/$C_2N_xO_{1-x}$-15 membrane, e, j) PIM-1/$C_2N_xO_{1-x}$-20 membrane (the insert images are the digital photos of the corresponding membranes)

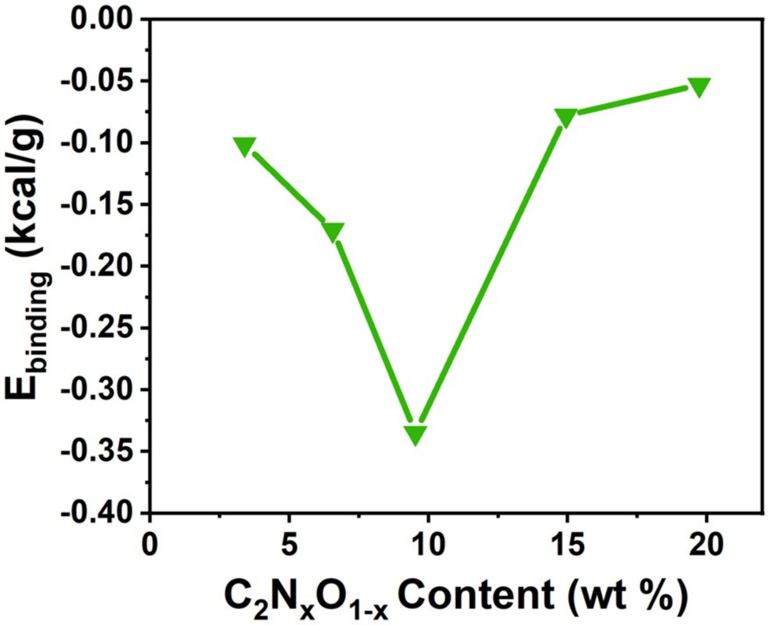

Fig. S5 Changes of binding energy between $C_2N_xO_{1-x}$ and PIM-1 in membrane with different concentrations of $C_2N_xO_{1-x}$.

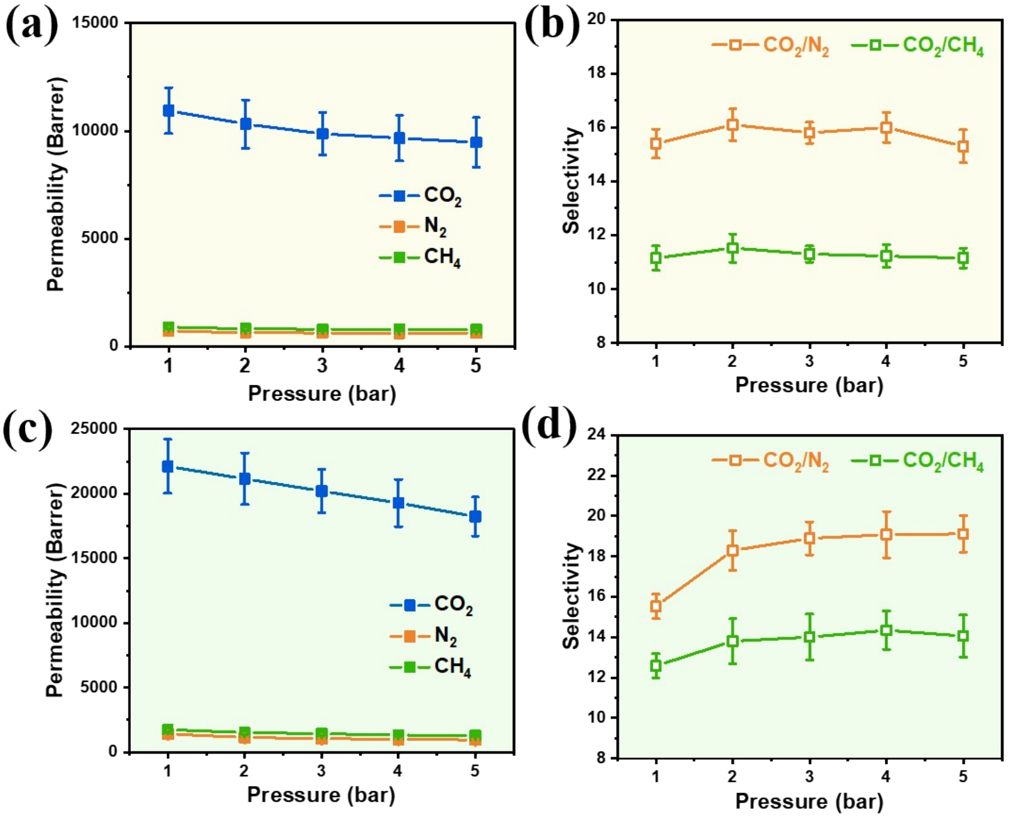

Fig. S6 The effect of operating pressure on the PIM-1 membrane a, b); PIM-1/$C_2N_xO_{1-x}$-10 membrane. c, d)

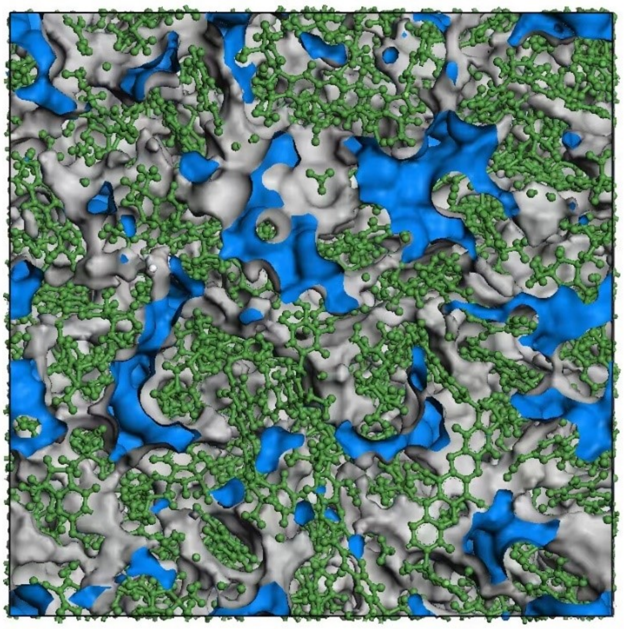

Fig. S7 Free volume elements in the PIM-1 model. Green represents the PIM-1 chains, the blue area represents the surface of free volume through the pore channel, and the grey area represents the pore volume.

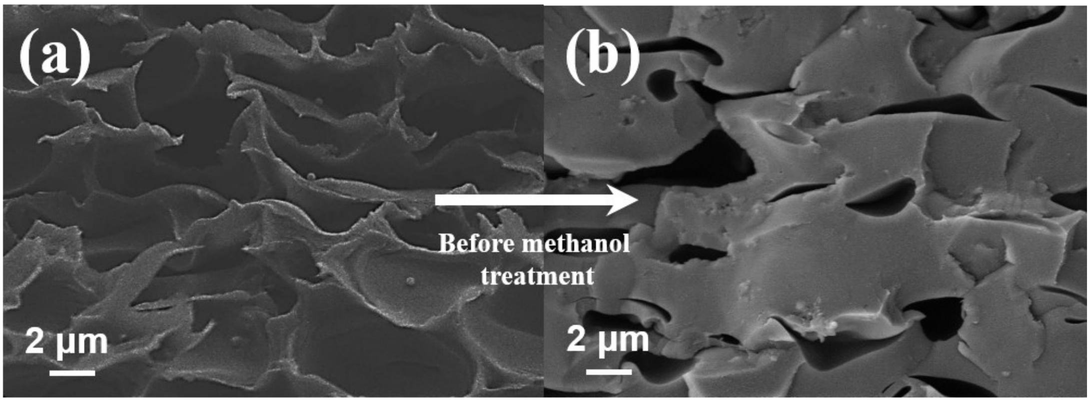

Fig. S8 The cross-section of P-PIM-1/$C_2N_xO_{1-x}$-10% membrane.

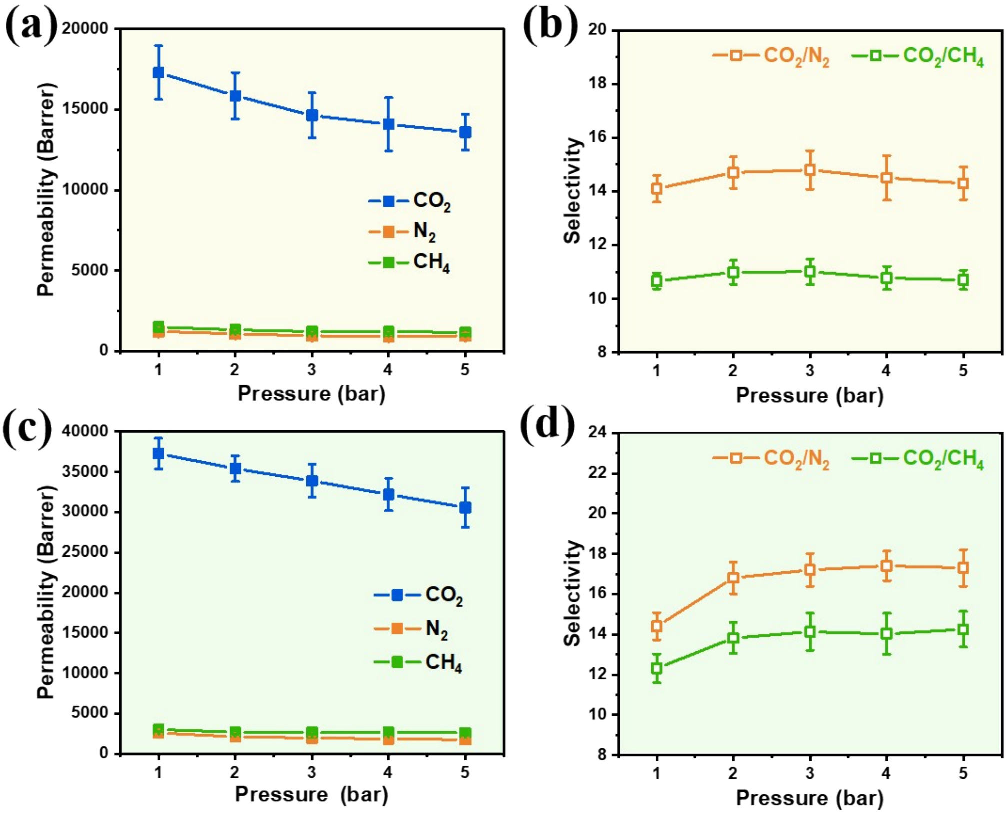

Fig. S9 The effect of operating pressure on the P-PIM-1 membrane a, b) and P-PIM-1/$C_2N_xO_{1-x}$-10 membrane c, d).

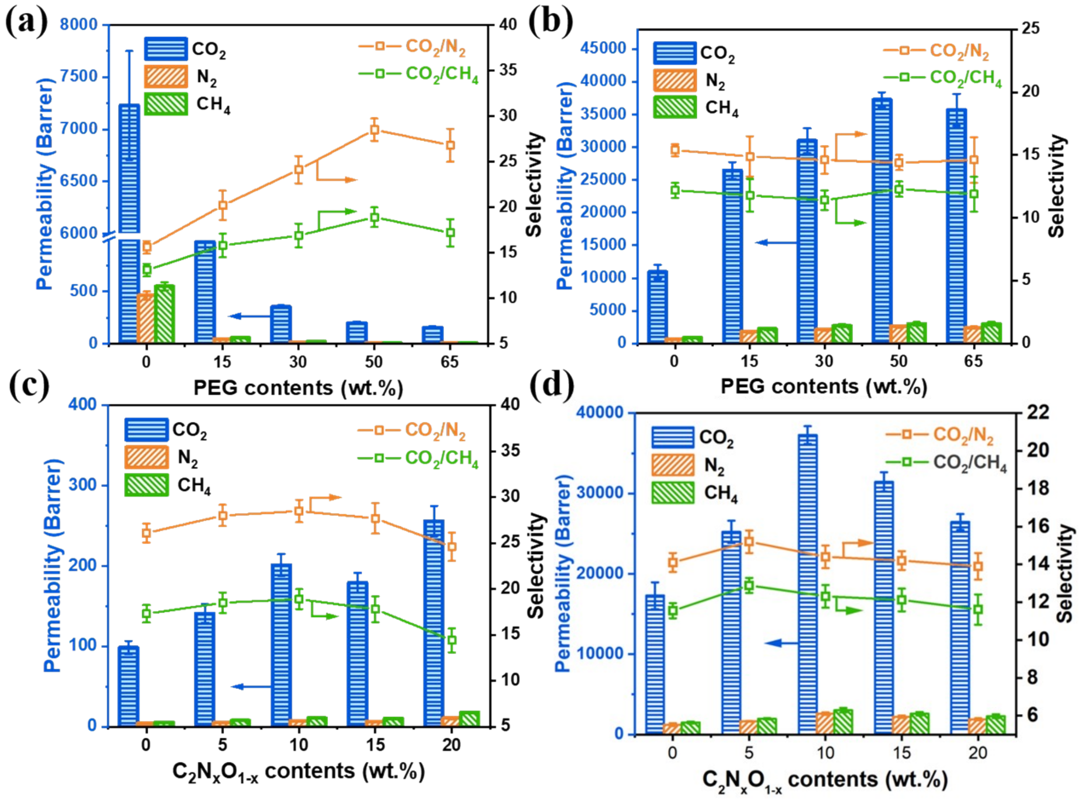

Fig. S10 a, b) The separation performance of PIM-1/PEG membrane with varying content of PEG-200 before and after methanol activation. c, d) The separation performance of P-PIM-1/C$_2$N$_x$O$_{1-x}$ membrane with different loading of C$_2$N$_x$O$_{1-x}$ before and after methanol activation.

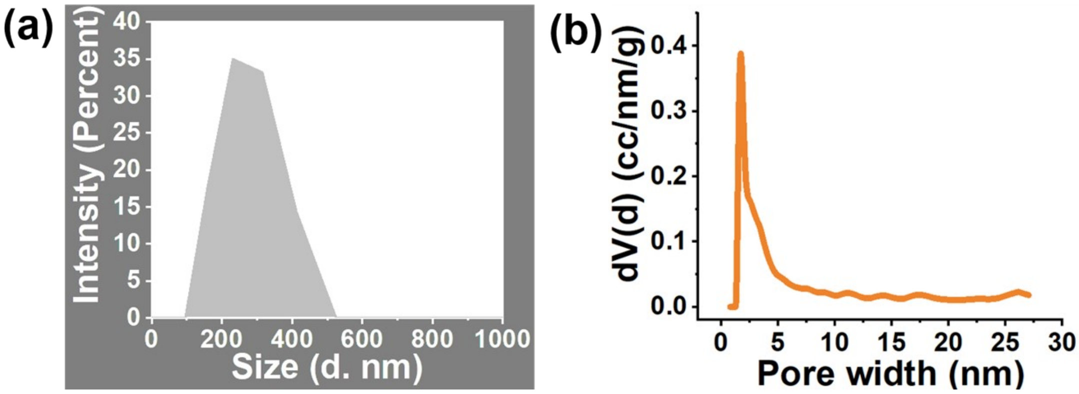

Fig. S11 a) Particle size distribution of C$_2$N$_x$O$_{1-x}$ by nanoparticle size analyzer. b) Pore size distribution of C$_2$N$_x$O$_{1-x}$ (The insets in Fig. 1c and 1e)

Part II: Supporting Tables

Table S1 The computed solubility, diffusivity, and corresponding selectivity of CO$_2$ and N$_2$ with changing the concentration of C$_2$N$_x$O$_{1-x}$.

$C_2N_xO_{1-x}$ wt%	S_{CO2} ($cm^3cm^{-3}cmHg^{-1}$)	S_{N2} ($cm^3cm^{-3}cmHg^{-1}$)	S_{CO2}/S_{N2}	D_{CO2} (*$10^{-7}cm^2/s$)	D_{N2} (*$10^{-7}cm^2/s$)	$D_{CO2/DN2}$
0	0.5469	0.0319	17.1337	8.0333	7.1333	1.1262
3.39	0.5490	0.0318	17.2412	8.9667	17.7000	0.5066
6.56	0.5717	0.0324	17.6628	11.3000	21.6500	0.5219
9.53	0.5919	0.0328	18.0202	15.8833	26.4667	0.6001
14.94	0.5418	0.0344	15.7607	8.1500	16.9500	0.4808
19.73	0.4859	0.0350	13.8972	5.7333	1.4133	0.4057

Table S2 Summary of compositions in each membrane model

$C_2N_xO_{1-x}$ -wt%	# of PIM-1	# of $C_2N_xO_{1-x}$	# of CO_2	# of N_2
0	20 chains / 10 monomers per chain	0	79	31
3.39		5	86	36
6.56		10	89	37
9.53		15	85	36
14.94		25	88	38
19.73		35	98	43

Table S3 Summary of the data in Fig. 4b

Membrane name	P_{CO2}（Barrer）	$\alpha_{CO2/N2}$	$\alpha_{CO2/CH4}$	Ref
Pebax®1657/30% O_2-BIT-72	145	66.2	/	1
PIM-1/HCP	19086	11.55	/	2
PIM-1/HCP	7159	21.11	/	2
PIM-1/HCP	9972	20.27	/	2
SPEEK/SiO_2-N-20	1321	54.2	/	3
PAO-PIM-1/NH_2-UiO-66 (30%)	8425	27.5	/	4
MOF-801/PIM-1%	6609	23	/	5
MOF-801/PIM-3%	7278	23.5	/	5
MOF-801/PIM-5%	9686	27	/	5
P8NP0.5	135	53	/	6
PIM-1/ZIF-8 28vol%	4270	21.89	/	7
PIM-1/ZIF-8 43vol%	6820	17.9	/	7
PIM-1/ZIF-8 11vol%	4825	19.3	/	7
PIM−1/SNW−1(10)	7553	22.7	/	8
PIM−1/SNW−1(5)	6080	21.7	/	8
PIM−1/SNW−1(15)	7954	19.9	/	8
0.4wt% COF-5/Pebax	493	49.3	/	9
Pebax−NC-30	1993	60	/	10

Pebax–NC-20	1431	69	/	10
PIM-1/PAF-1	3250	22	/	11
20 wt% ZIF-8/Pebax	180	41	/	12
PEBA2533-MMT-HD702 -PEG5000−40	448.5	70.7	/	13
PIM-10 ZIF	4271	/	11.3	14
PIM-20 ZIF	5942	/	11.9	14
PIM-30 ZIF	8377	/	11.2	14
SPEEK/SiO_2-N-20	2043	/	64.5	3
PIM-1/UiO-66(Zr) 16.6 wt%	9980	/	17.06	15
PIM-1/UiO-66(Zr) $(CO_2H)_2$ 28.6 wt%	9020	/	13.5	15
PIM-1/UiO-66(Zr)-NH_2 16.6 wt%	10700	/	13.6	15
PPU-2	369.3	/	31.3	16
PPUN-1.5	393.4	/	39.8	16
PPU-2	212.6	/	22.6	16
PPUN-1.5	245.3	/	29.4	16
PPU-2	242.5	/	26.4	16
PPUN-1.5	278.4	/	33.7	16
PIM−1/SNW−1(2)	5236	/	11.8	8
PIM−1/SNW−1(5)	6080	/	11.8	8
PIM−1/SNW−1(10)	7553	/	13.5	8
PIM-1/ZIF-8 43vol%	6300	/	14.7	7
BNN-PIM-0.8 wt%	3331	/	11.98	17
IL@COF-300/Pebax(7)	1601	/	39.5	18
COF-300/Pebax(7)	1268.	/	30.7	18

Reference of Table S3

1. N. Tara, Z. Shamair, N. Habib, M. Craven, M. R. Bilad, M. Usman, X. Tu and A. L. Khan, *Chem.Eng.Res.Des.*, 2022, **178**, 136-147.
2. T. Mitra, R. S. Bhavsar, D. J. Adams, P. M. Budd and A. I. Cooper, *Chem. Commun.*, 2016, **52**, 5581-5584.
3. Q. Xin, Y. Zhang, Y. Shi, H. Ye, L. Lin, X. Ding, Y. Zhang, H. Wu and Z. Jiang, *J. Membr. Sci.*, 2016, **514**, 73-85.
4. Z. Wang, H. Ren, S. Zhang, F. Zhang and J. Jin, *J Mater. Chem. A*, 2017, **5**, 10968-10977.
5. W. Chen, Z. Zhang, L. Hou, C. Yang, H. Shen, K. Yang and Z. Wang, *Sep. Purifi. Technol.*, 2020, **250**.
6. M. Asghari, M. Sheikh and M. Dehghani, *J. Chem. Technol. Biot.*, 2018, **93**, 2602-2616.
7. A. F. Bushell, M. P. Attfield, C. R. Mason, P. M. Budd, Y. Yampolskii, L. Starannikova, A. Rebrov, F. Bazzarelli, P. Bernardo, J. Carolus Jansen, M. Lanč, K. Friess, V. Shantarovich, V. Gustov and V. Isaeva, *J. Membr. Sci.*, 2013, **427**, 48-62.
8. X. Wu, Z. Tian, S. Wang, D. Peng, L. Yang, Y. Wu, Q. Xin, H. Wu and Z. Jiang, *J. Membr. Sci.*, 2017, **528**, 273-283.
9. K. Duan, J. Wang, Y. Zhang and J. Liu, *J. Membr. Sci.*, 2019, **572**, 588-595.
10. H. Zhang, R. Guo, J. Zhang and X. Li, *ACS Appl. Mater. Interfaces*, 2018, **10**, 43031-43039.

11. C. H. Lau, K. Konstas, A. W. Thornton, A. C. Liu, S. Mudie, D. F. Kennedy, S. C. Howard, A. J. Hill and M. R. Hill, *Angew. Chem. Int. Ed.*, 2015, **54**, 2669-2673.
12. P. D. Sutrisna, J. Hou, H. Li, Y. Zhang and V. Chen, *J. Membr. Sci.*, 2017, **524**, 266-279.
13. L. Dong, C. Zhang, Y. Bai, D. Shi, X. Li, H. Zhang and M. Chen, *ACS Sustainable Chem. Eng.*, 2016, **4**, 3486-3496.
14. L. Hao, K.-S. Liao and T.-S. Chung, *J Mater. Chem. A*, 2015, **3**, 17273-17281.
15. M. R. Khdhayyer, E. Esposito, A. Fuoco, M. Monteleone, L. Giorno, J. C. Jansen, M. P. Attfield and P. M. Budd, *Sep. Purifi. Technol.*, 2017, **173**, 304-313.
16. M. Mozafari, R. Abedini and A. Rahimpour, *J Mater. Chem. A*, 2018, **6**, 12380-12392.
17. A. W. Ameen, J. Ji, M. Tamaddondar, S. Moshenpour, A. B. Foster, X. Fan, P. M. Budd, D. Mattia and P. Gorgojo, *J. Membr. Sci.*, 2021, **636**.
18. R. Zhao, H. Wu, L. Yang, Y. Ren, Y. Liu, Z. Qu, Y. Wu, L. Cao, Z. Chen and Z. Jiang, *J. Membr. Sci.*, 2020, **600**.

Table S4 The comparison of the performance of the PIM-1 in this study with the reports in literature.

Name	P_{CO2} (Barrer)	$\alpha_{CO2/N2}$	$\alpha_{CO2/CH4}$
Ref. 1	11200	/	9.6
Ref. 2	9924	/	12.5
Ref. 3	8107	18.9	/
Ref. 4	8210	21.2	/
Ref. 5	8350	17.2	/
Ref. 6	8200	21.2	/
This work	10940	15.4	12.2

As we can see from Table S4, the performance of the PIM-1 in this study is similar with the reports in literature.

References

1. P. Budd, N. McKeown, B. Ghanem, K. Msayib, D. Fritsch, L. Starannikova, N. Belov, O. Sanfirova, Y. Yampolskii and V. Shantarovich, J. Membr. Sci., 2008, 325, 851-860.
2. M. M. Khan, S. Shishatskiy and V. Filiz, Membranes (Basel), 2018, 8.
3. S. Mohsenpour, A. W. Ameen, S. Leaper, C. Skuse, F. Almansour, P. M. Budd and P. Gorgojo, Sep. Purif. Technol., 2022, 298.
4. M. R. Khdhayyer, E. Esposito, A. Fuoco, M. Monteleone, L. Giorno, J. C. Jansen, M. P. Attfield and P. M. Budd, Sep. Purif. Technol., 2017, 173, 304-313.
5. P. F. Muldoon, S. R. Venna, D. W. Gidley, J. S. Baker, L. Zhu, Z. Tong, F. Xiang, D. P. Hopkinson, S. Yi, A. K. Sekizkardes and N. L. Rosi, ACS Materials Letters, 2020, 2, 821-828.
6. M. Khdhayyer, A. F. Bushell, P. M. Budd, M. P. Attfield, D. Jiang, A. D. Burrows, E. Esposito, P. Bernardo, M. Monteleone, A. Fuoco, G. Clarizia, F. Bazzarelli, A. Gordano and J. C. Jansen, Sep. Purif. Technol., 2019, 212, 545-554.

References

[1] S. Shenogin,. R. Ozisik, Xenoview at http://xenoview.mat.rpi.edu/, **2010**.

[2] J.R. Maple, M.-J. Hwang, T.P. Stockfisch, U. Dinur, M. Waldman, C.S. Ewig, A.T. Hagler, *J. Comput. Chem.* **1994**, 15, 162.

[3] Balçık M, Tantekin-Ersolmaz S B, Pinnau I, et al. *J. Mem. Sci.* **2021**, 640, 119838.

[4] Z. Tian, N. Fechler, M. Oschatz, T. Heil, J. Schmidt, S. Yuan, M. Antonietti, *J. Mater. Chem.* **2018**, 6, 19013.

[5] S. Plimpton, P. Crozier, A. Thompson, Lammps-large-scale atomic/molecular massively parallel simulator, Sandia National Laboratories. **2007**, 18, 43.

[6] D. Li, K. Panchal, R. Mafi, L. Xi, *Macromolecules* **2018**, 51, 6997.

[7] D. Li, K. Panchal, Vasudevan N K, et al. *Chem. Eng. Sci.* **2022**, 249: 117334.

[8] Budd P M, McKeown N B, Fritsch D. *Macromolecular Symposia. Weinheim: WILEY-VCH Verlag*, **2006**, 245, 403.

[9] L. Zhao, D. Zhai, B. Liu, Z. Liu, C. Xu, W. Wei, Y. Chen, J. Gao, *Chem. Eng. Sci.* **2012**, 68, 101.

[10] Fang W, Zhang L, Jiang J. *Mol. Simul.* **2010**, 36, 992.

[11] Hölck O, Böhning M, Heuchel M, et al. *J. Mem. Sci.* **2013**, 428, 523.

[12] Sekizkardes A K, Budhathoki S, Zhu L, et al. *J. Mem. Sci.* **2021**, 640, 119764.

[13] T. H. Lee, A. Ozcan, I. Park, et al. *Adv. Funct. Mater*. **2021**, 31(38): 2103973.

[14] Budd P M, McKeown N B, Fritsch D. *J. Mater. Chem.* **2005**, 15, 1977.

[15] Swaidan R, Ghanem B, Litwiller E, et al. *Macromolecules*, **2015**, 48, 6553.

[16] Gonciaruk A, Althumayri K, Harrison W J, et al. *Microporous Mesoporous Mater.* **2015**, 209, 126.

[17] W. Zou, G. Jiang, W. Zhang, et al. *Adv. Funct. Mater*. **2023**: 2213642.

[18] B. Zheng, X. Lin, X. Zhang, et al. *Adv. Funct. Mater*. **2020**, 30(41): 1907006.

[19] C. R. Mason, L. Maynard-Atem, K. W. Heard, B. Satilmis, P. M. Budd, K. Friess, M. Lanč, P. Bernardo, G. Clarizia and J. C. Jansen, Macromolecules, **2014**, 47, 1021-1029.

[20] P. Sarrami and M. Movahedi, Computational Materials Science, **2022**, 207.

[21] L. Hou, Z. Wang, Z. Chen, W. Chen and C. Yang, Sep. Purif. Technol., **2020**, 242.

[22] P. F. Muldoon, S. R. Venna, D. W. Gidley, J. S. Baker, L. Zhu, Z. Tong, F. Xiang, D. P. Hopkinson, S. Yi, A. K. Sekizkardes and N. L. Rosi, ACS Materials Letters, **2020**, 2, 821-828.

[23] J. M. Luque-Alled, M. Tamaddondar, A. B. Foster, P. M. Budd and P. Gorgojo, ACS Appl. Mater. Interfaces, **2021**, 13, 55517-55533.